






Triode magnetron injection gun for the KIT 2 MW 170 GHz coaxial cavity gyrotron

Cite as: Phys. Plasmas **27**, 023105 (2020); <https://doi.org/10.1063/1.5132615>

Submitted: 18 October 2019 . Accepted: 20 January 2020 . Published Online: 05 February 2020

Ioannis Gr. Pagonakis, Konstantinos A. Avramidis , Gerd Gantenbein, Stefan Illy, Zisis C. Ioannidis , Jianbo Jin, Parth Kalaria , Bernhard Piosczyk, Sebastian Ruess, Tobias Ruess, Tomasz Rzesnicki, Manfred Thumm , and John Jelonnek 



View Online



Export Citation



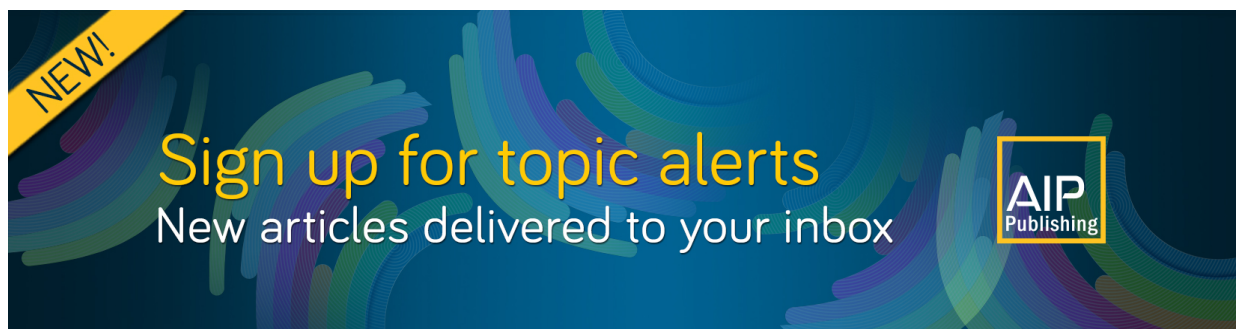
CrossMark

ARTICLES YOU MAY BE INTERESTED IN

[Coaxial multistage depressed collector design for high power gyrotrons based on E×B concept](#)
Physics of Plasmas **26**, 113107 (2019); <https://doi.org/10.1063/1.5118338>

[Enhancement-limit of Smith–Purcell radiation with self-bunched keV-order electron beam](#)
Physics of Plasmas **27**, 023102 (2020); <https://doi.org/10.1063/1.5126364>

[Electron self-injection threshold for the tandem-pulse laser wakefield accelerator](#)
Physics of Plasmas **27**, 023106 (2020); <https://doi.org/10.1063/1.5117503>



NEW!
Sign up for topic alerts
New articles delivered to your inbox
AIP
Publishing



Triode magnetron injection gun for the KIT 2 MW 170 GHz coaxial cavity gyrotron

Cite as: Phys. Plasmas **27**, 023105 (2020); doi: [10.1063/1.5132615](https://doi.org/10.1063/1.5132615)

Submitted: 18 October 2019 · Accepted: 20 January 2020 ·

Published Online: 5 February 2020



View Online



Export Citation



CrossMark

Ioannis Gr. Pagonakis,^{a)} Konstantinos A. Avramidis,  Gerd Gantenbein, Stefan Illy, Zisis C. Ioannidis,  Jianbo Jin, Parth Kalaria,  Bernhard Piosczyk, Sebastian Ruess, Tobias Ruess, Tomasz Rzesnicki, Manfred Thumm,  and John Jelonnek 

AFFILIATIONS

Karlsruhe Institute of Technology (KIT), IHM, 76131 Karlsruhe, Germany

^{a)} Author to whom correspondence should be addressed: ioannis.pagonakis@kit.edu

ABSTRACT

Considering the recent understanding of the physics of electron trapping mechanisms taking place in the magnetron injection gun (MIG) region of gyrotrons and the sensitivity of the emitter ring manufacturing tolerances on the electron beam quality, a MIG has been designed and manufactured for the 2 MW, 170 GHz coaxial cavity gyrotron developed at Karlsruhe Institute of Technology. The new MIG has the following novelties: (i) the design satisfies the criteria for the suppression of the electron trapping mechanisms, (ii) a new type of emitter ring is used for the suppression of the influence of the manufacturing tolerances and misalignments on the quality of the generated electron beam, and (iii) the design was optimized to generate a good beam quality in a wide variety of magnetic field profiles to increase the flexibility. An additional important feature of the new triode MIG design is the possibility to operate with only two power supplies by using a special start-up scenario. The first experimental results of the coaxial cavity gyrotron with the new MIG are presented.

Published under license by AIP Publishing. <https://doi.org/10.1063/1.5132615>

I. INTRODUCTION

It has been theoretically shown¹ that the presence of longitudinal corrugation on the insert of the coaxial cavity gyrotron^{2,3} supports the excitation and stability of a very high order mode against the dramatic increase in competitor modes. Based on that theoretical evidence, a significant effort took place during the last two decades in the development of a 2 MW, 170 GHz coaxial cavity gyrotron with nominal mode TE_{34,19}.^{4,5,7} The most remarkable results of the coaxial cavity gyrotron were a 2.2 MW record output power without depression and an output power on the order of 1.9 MW with an overall efficiency of 48% with depressed collector operation.^{6,7} The pulse length was limited in the range of a few ms due to the fact that, for the pulse extension to a range of several tenths of milliseconds, cooling is necessary for the critical gyrotron subcomponents such as beam-tunnel, cavity, output coupler, beam tunnel, and collector. In the short-pulse prototype, except the oil cooled electron gun, the water cooling applied on the coaxial insert, and a primitive water cooling of the collector to increase the duty cycle, no other gyrotron subcomponent is cooled. A significant effort has taken place during the last two years at Karlsruhe Institute of Technology (KIT) in order to upgrade the technological design of the critical gyrotron subcomponents with a water cooling in order to support a pulse length extension to the range of 100 ms.^{8,9} In parallel, an improved

magnetron injection gun (MIG) has been designed at KIT and manufactured by the industrial partner Thales Electron Devices (TED).

For the design of the new MIG, the recent understanding in high power gyrotron MIG physics achieved during the last decade in the context of development of the 2 MW coaxial¹⁰ and the 1 MW conventional¹¹ cavity 170 GHz European (EU) gyrotrons for ITER has been considered. A series of issues related to MIG physics has been comprehensively studied, such as the electron trapping mechanisms in the MIG and the sensitivity of the electron beam quality on the manufacturing tolerances and misalignments in the emitter ring region.

In particular, during the experimental campaign of the first industrial prototype of the coaxial cavity gyrotron,¹² substantial effects of the trapped electrons on the gyrotron operation have been identified.¹³ Voltage stand-off instabilities and periodic appearance of a significant leakage current on the electrodes were encountered during voltage stand-off tests, while unstable operation even in very short pulses in the presence of the electron beam limited the power to significantly lower values than the expected one. During the internal inspection of the tube, after the end of the experiments, many electron traces were observed on the metallic surfaces. The investigation of this evidence showed that most of the observations were related to the presence of trapped electrons in the tube due to two different electron

trapping mechanisms: (i) the adiabatic trap due to the compression of the magnetic field from the cathode toward the cavity^{14,15} and (ii) the potential well trapping which is formed at some regions due to the geometry of MIG electrodes and the shape of the magnetic field lines. Two MIG design criteria have been defined in order to suppress the influence of these two electron trapping mechanisms on the gyrotron operation.¹⁶ The first design criterion imposes that all secondary electrons emitted from the overall cathode surface must not be adiabatically trapped. As it was theoretically shown, this criterion supports the suppression of the harmful beam halo, which could be generated in the magnetic compression region between the cathode and cavity, influencing the quality of the beam before it enters the interaction region. The second design criterion imposes that the geometry of the cathode and anode must prevent the formation of any magnetic potential well. Therefore, the possibility of the appearance of voltage stand-off instabilities in long-pulse operation related to the electron accumulation in a magnetic potential well in the MIG region is suppressed.

Other important issues are the manufacturing tolerances and possible misalignments in the emitter ring region. It was numerically identified that a minor misalignment of the emitter ring vs its neighboring parts on the order of few tens of micrometers could have a dramatic influence on the quality of the generated electron beam.¹⁷ In the same work, a new type of emitter ring with coated rims was proposed to significantly suppress that sensitivity.

Furthermore, the experimental campaigns of the short pulse^{18,19} and continuous wave²⁰ prototypes of the EU 170 GHz, 1 MW conventional cavity gyrotron for ITER, as well as older experiments²¹ with the coaxial cavity gyrotron at KIT, identified the importance of the possible operation of the MIG in a wide range of magnetic profiles. This flexibility is very important for the optimization of the gyrotron performance under the influence of many factors which are not taken into account during the design phase of the gyrotron, such as the manufacturing tolerances and the misalignment with the magnetic field. Based on that fact, an additional design criterion for the MIG was considered: The MIG must generate a high quality electron beam in a wide range of magnetic profiles.

All these theoretical and experimental results were taken into account for the design of an improved MIG, which was manufactured at TED and tested in short pulses at KIT. A more detailed analysis of the new MIG design²² is given in Sec. II. The first experimental results of the coaxial cavity gyrotron with the new MIG are presented in Sec. III, while a short summary of this work is presented in Sec. IV.

II. DESIGN

In this section, four important issues related to the new triode MIG design are presented: (i) the methodology used for the suppression of the electron trapping mechanisms in the MIG region is discussed in Sec. II A, (ii) the advantages of the edge coated emitter ring on the suppression of the influence of manufacturing tolerances and possible misalignments of the emitter ring vs its neighboring parts on the beam quality are discussed in Sec. II B, (iii) the parameters of the generated electron beam of the new MIG are presented in Sec. II C, and (iv) the possible gyrotron operation with two power supplies, instead of three required for gyrotrons with a triode magnetron injection gun, is theoretically discussed in Sec. II D.

A. Electron trapping

The presence of the insert in the coaxial cavity gyrotron causes several difficulties in the MIG design. The insert is fixed at the bottom part of the gyrotron and, therefore, it passes through the cathode. For this reason, the cathode has a coaxial geometry instead of the cylindrical one of conventional cavity gyrotrons. Since the body potential is also applied to the insert, a high electric field is generated in the inner and outer regions of the cathode. That electric field causes significant difficulties to satisfy the first design criterion for the suppression of the beam halo generation. The most critical area is the outer side of the cathode nose. During the design phase of a conventional diode type coaxial MIG, it was identified that there are many difficulties to suppress the beam halo emitted from the cathode nose. Due to the high electric field on the cathode nose, some of the secondary electrons emitted from that area have a significant initial transverse velocity which causes their adiabatic trapping in the region between the cathode and cavity.

In order to address that issue, two alternative design approaches were considered. In the first approach, the emission of the electron is inverted, i.e., the electrons are emitted radially inwards.^{23,24} As it is presented in Ref. 24, this design approach provides the necessary flexibility to avoid high electric field on the cathode regions and to satisfy the criterion related to the beam halo suppression. In the second approach, which is considered in this work, a triode configuration is used. The geometry of the modulation anode is optimized in such a way that the required electric field for the emission of the beam electrons with the desired properties is achieved locally at the emitter ring region, while keeping the electric field on the cathode nose surface in safe levels.

A three-dimensional representation of the MIG is presented in Fig. 1. The nominal operating parameters are summarized in Table I, while the nominal potential applied to the electrodes are presented in Table II. The closest distance between the anode and the cathode is placed at the emitter ring region. The electric field at that region has the required value for the generation of the appropriate beam while, in all other regions, it is kept as low as possible. The electric field at the outer side of the cathode nose, which is one of the most critical regions for the emission of potentially trapped secondary electrons, has a

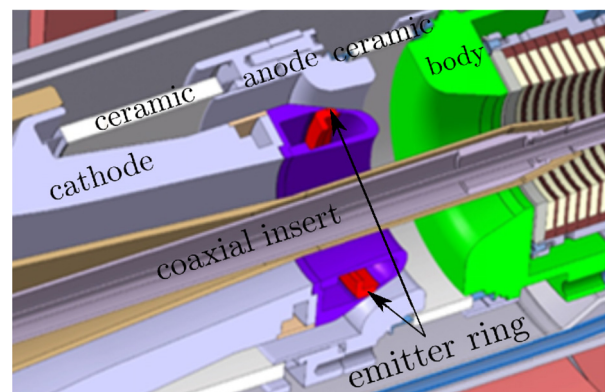


FIG. 1. A 3D-CAD drawing of the new triode MIG design. The electrode noted as "anode" corresponds to the modulation anode, while the electrode noted as "body" corresponds to the anode of the triode configuration.

TABLE I. Operating parameters.

Nominal cavity mode	TE _{34,19}
Frequency, f	170 GHz
Power, P	2 MW
Efficiency, η_t (with SDC)	50%
Magnetic field, B_c	6.86 T
Accelerating voltage, V_{acc}	90 kV
Depression voltage, V_{dep}	35 kV
Beam current, I_b	75 A
Beam radius, r_b	10.0 mm
Pitch factor, α	1.3
Transverse velocity spread, $\delta\beta_t$	<3%

TABLE II. Nominal potential of electrodes.

Cathode, V_c	-55 kV
Anode, V_a	0 kV (ground)
Body, V_b	+35 kV
Coaxial insert, V_i	+35 kV

maximum value in the range of 60 kV/cm, as shown in Fig. 2. It should be noted that, in the diode configuration, it is rather challenging to suppress that to values less than 75 kV/cm.

The secondary electrons emitted from the cathode surface in close vicinity to the emitter ring are guided by the magnetic field lines through the cavity toward the collector. These electrons are influenced by the magnetic compression, and they are candidates for adiabatic trapping. The critical area on the cathode surface where these secondary electrons are emitted is shown in Fig. 3. Secondary electrons emitted from the cathode surface away from the emitter guided by the magnetic field toward the anode, body, and coaxial insert without to enter to the magnetic compression region. As shown in Fig. 4, the pitch factor of the electrons emitted from the critical cathode area with zero initial velocity is less than the threshold $\alpha_{max} \approx 3$ (defined in Ref. 18). In this way, it is ensured that no true secondary electron emitted from the cathode surface is adiabatically trapped, suppressing the possibility of the generation of the harmful beam halo.

It should be also mentioned that the shape of the electrodes has been designed taking into account the second design criterion, which is related to the formation of the potential wells. Therefore, the design

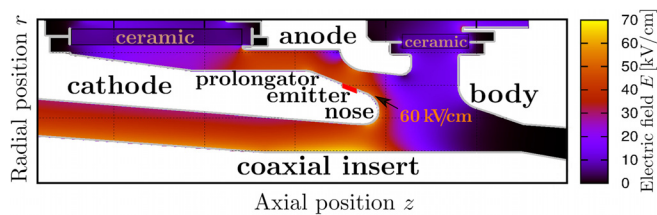


FIG. 2. Electric field in the MIG region.

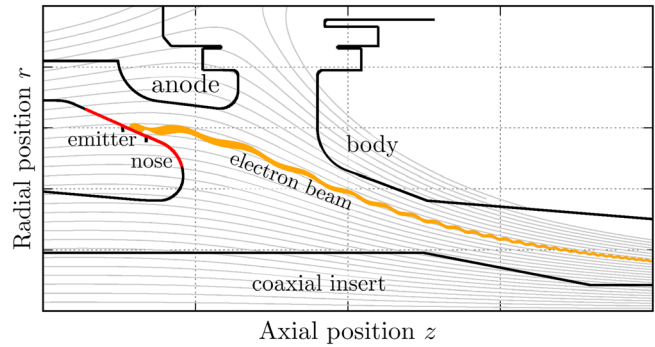


FIG. 3. Magnetic field lines (gray lines) guide the secondary electrons emitted away from the emitter ring toward the anode, body, and coaxial insert. The secondary electrons emitted from the area close to the emitter ring (indicated by the red line on the cathode surface) pass through the cavity toward the collector.

of the new MIG ensures that no electrons are trapped in the MIG region due to this mechanism.

B. Emitter ring sensitivity

It has been theoretically shown that a possible misalignment of the emitter ring vs its neighboring parts (cathode nose and prolongator) could have dramatic effects on the beam quality. In particular, a minor radial shift of the emitter ring causes a significant variation of the average pitch factor, a significant increase in the velocity spread, and a harmful long tail at the high value side of the pitch factor distribution. A novel type of emitter ring with anti-emission coating at the edge rims, shown in Fig. 5, has been proposed for the minimization of the influence of the manufacturing tolerances on the beam quality.¹⁷

The pitch factor variation $\Delta\alpha$ as a function of the radial shift Δr is presented in Fig. 6 for several values of the axial extension Δz_c of the coated emitter ring area. It is remarkable that as the coated extension

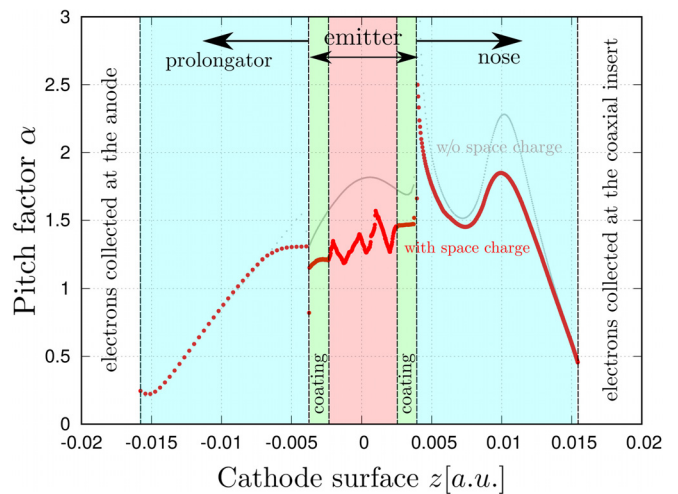


FIG. 4. Pitch factor at the cavity of the electrons emitted from the critical area of the cathode surface with zero initial velocity. The maximum value of pitch factor is less than the threshold, $\alpha_{max} \approx 3$.

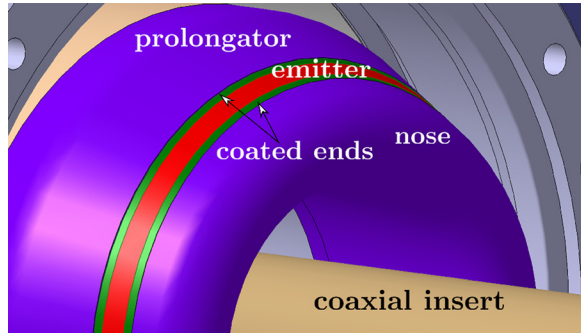


FIG. 5. Emitter ring with coated rims.

Δz_c is increasing, the slope of the pitch factor variation curve is decreasing approaching the horizontal line which represents that case for which the pitch factor is completely insensitive to the radial deviation. In Table III, the sensitivity factor s , which represents the ratio of the pitch factor variation $\Delta\alpha$ to the radial shift Δr , and the relative suppression of the sensitivity δs for several values of the coated axial extension Δz_c are presented.

It is remarkable that for the new triode MIG, a significant longer coating extension Δz_c is required to suppress that sensitivity in comparison to the conventional MIG of the cylindrical cavity gyrotron for ITER. In particular, the sensitivity factor s was reduced from 1.83/mm to 0.55/mm for $\Delta z_c = 1$ mm at the diode MIG design,¹⁷ while in the triode MIG presented here, in order to lower the sensitivity s at a similar level from 1.95/mm to 0.60/mm, a double coating extension $\Delta z_c = 3$ mm is required. A possible explanation for that fact is that this sensitivity is correlated with the electric field in the emitter ring region, which for the triode configuration is higher than the diode one.

The new type of emitter ring is being used in the new MIG. However, for the length of the coating, the conservative choice of $\Delta z_c = 1.5$ mm was realized. This choice ensures a significant decrease in the sensitivity factor, while the emitter ring thickness Δz_e is kept in a

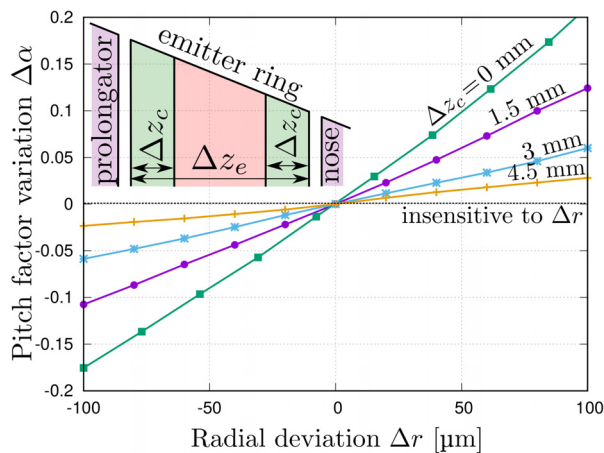


FIG. 6. Pitch factor variation $\Delta\alpha$ as a function of the emitter ring radial deviation Δr for several values of the axial extension Δz_c of the anti-emission coated emitter ring area.

TABLE III. Sensitivity factor vs the length of the coated area.

Δz_c (mm)	Δz_e (mm)	s (1/mm)	δs
0	4.5	1.95	...
1.5	7.5	1.16	40.5%
3	10.5	0.60	69.2%
4.5	13.5	0.26	86.7%

value closer to the conventional emitter. It should be pointed out that such a type of emitter ring has been already tested in a low beam current ($I_b = 0.5$ A) MIG of a low power and high frequency gyrotron.²⁶

C. Beam parameters

For the design of the new MIG, the possibility to generate a high quality electron beam in a wide range of magnetic profiles was considered. This is quite important for the optimization of the gyrotron performance during the experiments considering several factors which could influence the gyrotron operation, such as parasitic oscillations and manufacturing tolerances. As it is discussed in Ref. 25, the three important parameters of the magnetic profiles are (i) the value of the magnetic field B_c in the cavity, (ii) the magnetic compression, which determines the beam radius in the cavity, and (iii) the magnetic field angle at the emitter which influences the beam laminarity. The geometry of the MIG was optimized in order to achieve a high quality beam in a wide range of beam radius r_b in the cavity and magnetic field angles φ_B at the emitter.

In Fig. 7, two important parameters of the electron beam are plotted in a wide range of magnetic compression and magnetic field angle at the emitter. The average pitch factor α is shown at top and the transverse velocity spread $\delta\beta_t$ at bottom. The pitch factor significantly increases with the decrease in the beam radius in the cavity, as expected, due to the larger magnetic compression, while it is not significantly influenced by the magnetic field angle φ_B . At the nominal point ($\varphi_B = 0^\circ$, $r_b = 10.0$ mm), the pitch factor is slightly higher than 1.3. The velocity spread is quite low in a wide range of the theoretical map as shown at the bottom of Fig. 7. The speed is dramatically increased only for angles $\varphi_B < -4^\circ$. Therefore, for a wide range of parameters, the beam quality is quite good. Therefore, a large number of magnetic profiles can be used during the experiments for the optimization of the gyrotron performance.

D. Operation

The new MIG has a triode configuration in order to suppress the possible adiabatic trapping of the secondary electrons emitted from the cathode nose. The triode configuration provides an additional flexibility in the gyrotron operation since it is possible to adjust independently the pitch factor, the beam energy, and the spent beam deceleration voltage. The operation of the gyrotron with a triode MIG requires three power supplies: cathode V_c , body V_b , and anode V_a . The accelerating voltage is given by the difference $V_{acc} = V_b - V_c$, the depression voltage applied on the spent beam at the entrance of the grounded collector is $V_{dep} = V_b$, while using the anode potential, it is possible to adjust the electric field in the emitter ring region and, therefore, the pitch factor of the electron beam.

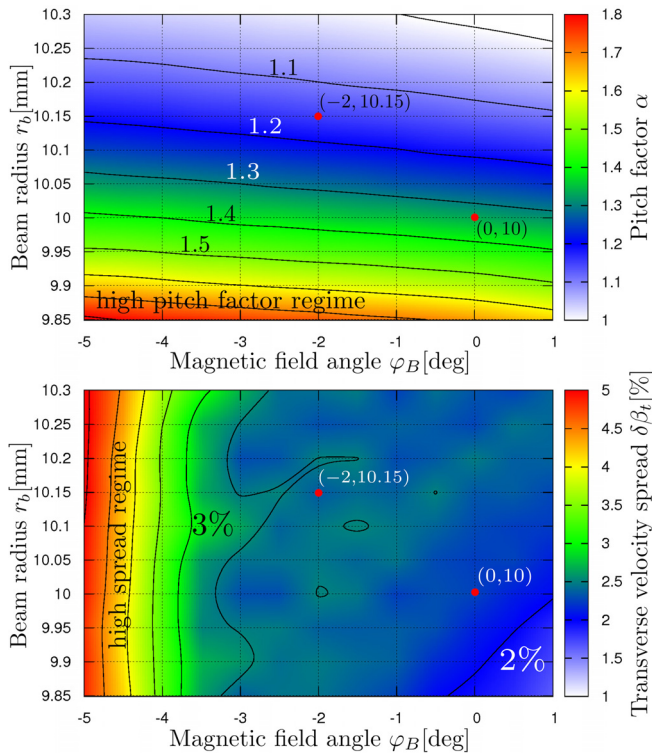


FIG. 7. The average pitch factor α (top) and transverse velocity spread $\delta\beta_t$ (bottom) of the electron beam in the center of the cavity as functions of the magnetic profile, defined by the magnetic field angle φ_B at the emitter, and the magnetic compression which is equivalent to the beam radius r_b in the center of the cavity.

An additional feature of the new MIG is that it can also operate with only two power supplies. This is possible due to the fact that the nominal anode potential V_a was set to be zero (grounded). Therefore, to apply the nominal potential on the anode, no additional power supply is required. In order to operate the gyrotron, under this configuration, the cathode and body voltages should be properly modulated during the pulse. Figure 8 depicts such a ramp-up scenario that consists of two steps. At the first step, the slow body power supply is activated to the nominal body voltage, and at the second step, the fast cathode power supply is also activated. It is remarkable that, during the time that the body power supply is activated, a negligible current is expected due to the fact that the electric field in the emitter ring region is very low.

A simple approach is discussed here in which it is possible to adjust the pitch factor α keeping the accelerating voltage V_{acc} constant using only two power supplies. For instance in order to increase the pitch factor independently of the accelerating voltage, it is necessary to increase the electric field in the emitter ring region. Therefore, a higher voltage between the cathode and the anode electrode is required. Since the anode is grounded, the only way to achieve that is to reduce the cathode potential by $\Delta V > 0$ to more negative values. In parallel, in order to keep the accelerating voltage constant, the body voltage must be decreased by ΔV . The variation of the pitch factor and the velocity spread for several values of the cathode and body potential for the nominal magnetic field are shown in Fig. 9. It is remarkable that the

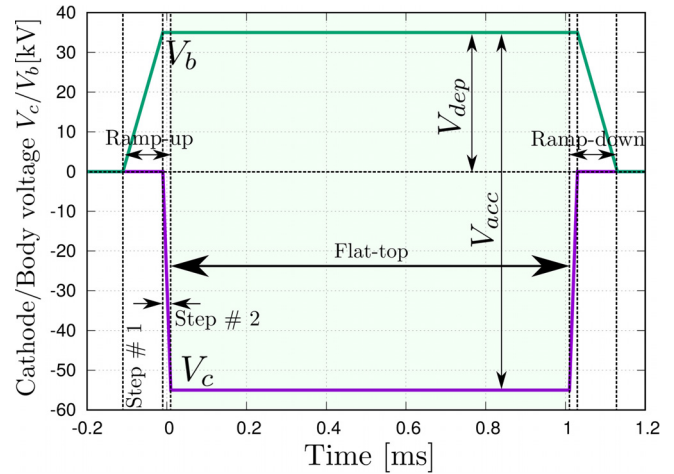


FIG. 8. Modulation of the cathode and body potential during a short pulse.

pitch factor significantly varies for a small variation of the cathode and body potential. For a voltage variation $\Delta V \pm 2$ kV, the pitch factor has the significant variation $\Delta\alpha \approx 0.4$, while the theoretical estimation of the overall gyrotron efficiency η_t is not significantly influenced as presented in Table IV. For the calculation of the overall efficiency, an interaction efficiency of 35% and losses of 10% were considered.

However, the absence of an additional power supply introduces an important constraint. The depression voltage cannot be optimized independently since it is equivalent to the body potential. Therefore, it should be ensured that a depression voltage equal to the body potential plus a reasonable margin of about 2 kV for the pitch factor adjustment possibility does not cause reflections of the slow electrons of the spent beam at the collector entrance. Theoretical and experimental studies of the coaxial cavity gyrotron with an older MIG justify that the choice of a nominal body voltage at $V_b = 35$ kV was considered as a reasonable option.²⁷

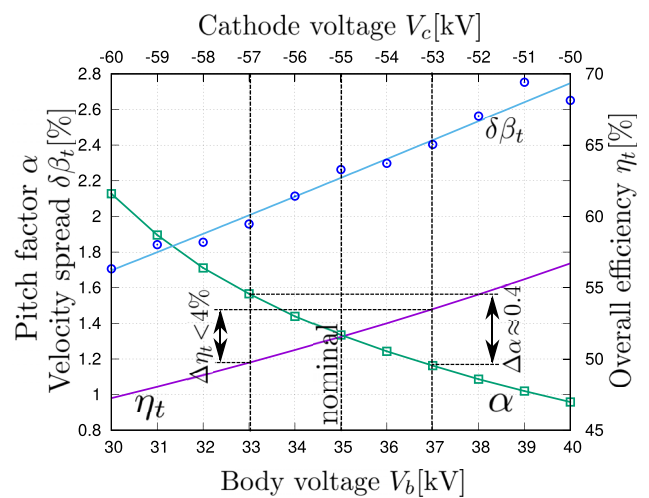


FIG. 9. Demonstration of the triode operation of the new MIG with two power supplies.

TABLE IV. Pitch factor and overall efficiency variations.

V_c (kV)	V_b (kV)	α	η_t
-57	33	1.56	49.7%
-56	34	1.44	50.6%
-55	35	1.33	51.5%
-54	36	1.24	52.5%
-53	37	1.16	53.4%

III. FIRST EXPERIMENTAL RESULTS

The new MIG has been manufactured by TED based on the design discussed in Sec. II. Then, it has been installed in the coaxial cavity gyrotron. Some preliminary experiments at a few milliseconds pulse duration were first conducted. During these experiments, an unexpected behavior of the beam current was observed. As shown in Fig. 10, the beam current was not constant as usual during the flat top of such a pulse length. In the first few milliseconds of the pulse, a strong variation of the beam current was observed, while after about 10 ms, the beam current was converging to a constant value.

The beam current behavior was comprehensively investigated for many operating parameters. It was concluded that the beam current variation is significantly influenced by the emitter ring filament current as shown in Fig. 11, where the absolute ΔI_b and the relative δI_b beam current variation during 2 ms pulses as functions of the filament current I_f are presented. On the other hand, the beam current variation was insensitive to the different magnetic field profiles and the different accelerating and decelerating voltages. A more comprehensive study is required in order to deeply understand the physics and the root cause of that unexpected behavior.

The strong beam current variation causes some difficulties to operate the tube stably in short pulses using the startup scenario discussed in Sec. IID. The current variation during the flat-top of the pulse has a strong influence on the generated mode, the output power,

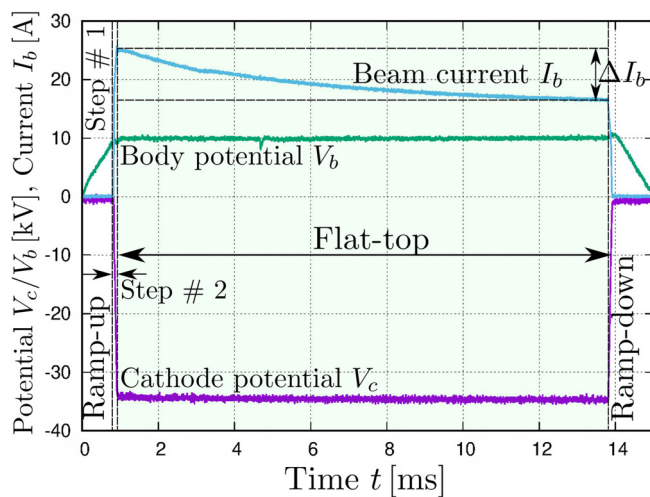


FIG. 10. Beam current variation during 14 ms pulse at down scaled operating parameters.

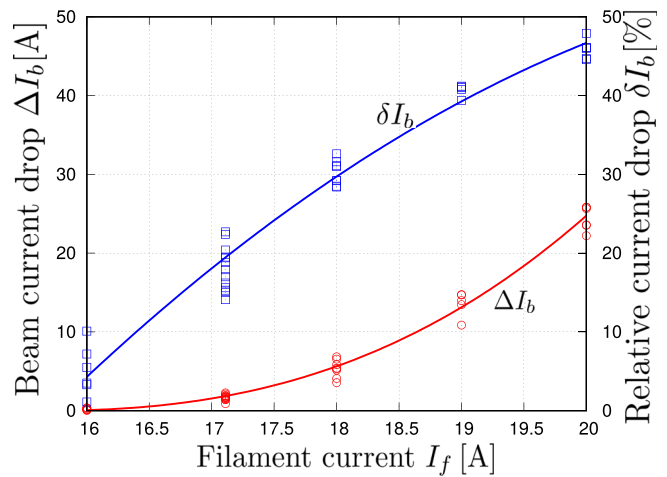


FIG. 11. Absolute ΔI_b and relative δI_b beam current variations during 2 ms pulses as functions of the emitter ring filament current I_f .

and the efficiency. However, it was possible to operate the tube in short pulse considering a more complicate startup scenario shown in Fig. 12. This scenario based on the experimental observation that if a smaller current than the nominal one is maintained for some time $\Delta t_d \approx 2 - 3$ ms before the flat-top, and then the current variation during the flat top is significantly reduced.

As shown in Fig. 12, initially the body voltage is set to 10 kV (step #1). During this step, no beam current was measured due to the very low electric field at the emitter, as already discussed. Then, the cathode potential slowly increases from zero to an intermediate potential in the range of -25 kV, significantly smaller in amplitude than the nominal value -55 kV (step #2). In parallel, the beam current gradually increases as usual passing through the space charge limited and the temperature limited regimes. In the same step, the body potential reaches its nominal value. It should be noted that the intermediate

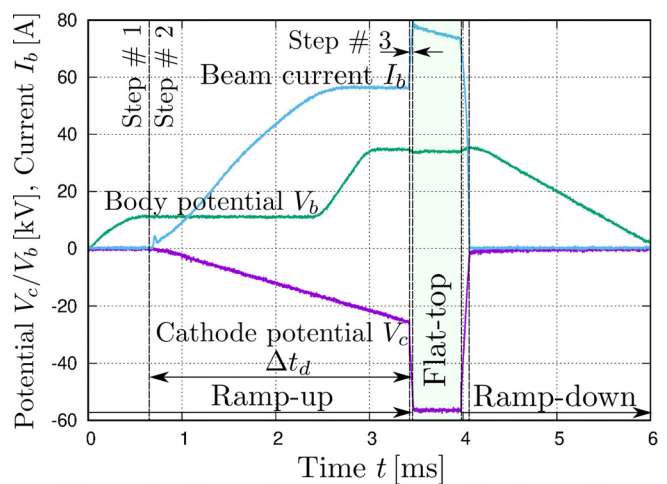


FIG. 12. Specific startup scenario used for the delay of the flat-top of the pulse in order to minimize the beam current variation.

cathode potential should be sufficiently small to avoid the excitation of any mode in the cavity. Finally, in the short step #3, the cathode potential also reaches its nominal value. During the half of millisecond flat-top period, the beam current variation is in the range of few amperes. Using this approach, the beam current flows through the tube for a significant time Δt_d before the flat top is reached. As a result, the beam current variation during the flat top is significantly reduced.

For the power measurement, the more accurate two pulses approach was considered. In particular, for each operating point, two successive pulses were performed with identical ramp-up and ramp down scenarios as shown in Fig. 12 for both pulses. However, the flat-top time in the first pulse was 0.5 ms while in the second one it was only 0.1 ms. The power of the pulse for any operating point was estimated by the ratio of the energy difference measured by the calorimeter to the flat-top time difference (0.4 ms). In this way, it was ensured that the small amount of energy which is generated during the long ramp-up does not influence the power measurement during the short flat-top of the pulse.

First, some experimental results were obtained using only two power supplies and the modulation anode at the ground potential. In Fig. 13, the measured power and efficiency of the coaxial cavity gyrotron are presented as a function of the accelerating voltage for three values of body potential: (i) 33 kV, (ii) 33.8 kV, and (iii) 34.4 kV. The maximum power was in the range of 1.95 MW, while the optimal efficiency was about 43%.

The possibility to use an additional power supply to get all the flexibility of the triode configuration was also shortly investigated. In particular, the modulation anode was connected with a simple DC, low power, commercial power supply available at KIT. Having no possibility to modulate the anode voltage during the pulse, the voltage was maintained before and after the pulses for long time. Due to the fact that the applied voltage to the anode was negative, no current was emitted from the cathode beside the real pulse. Using a similar start-up scenario as presented in Fig. 12, setting the cathode potential to $V_c = 63$ kV and the body potential to $V_b = 30$ kV, a constant accelerating voltage $V_{acc} = 93$ kV was applied to the electron beam with a current

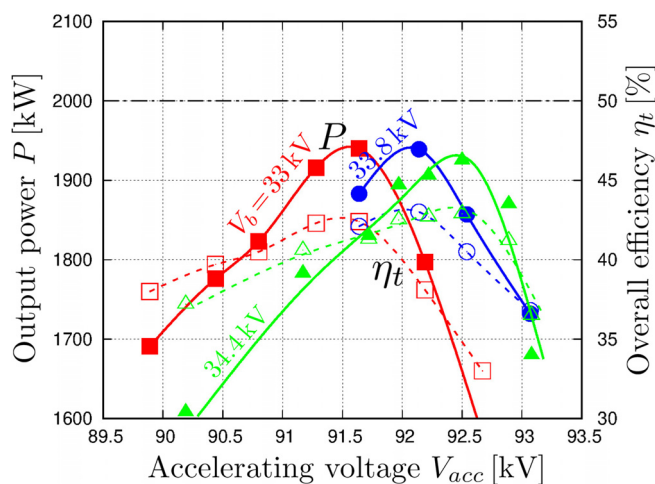


FIG. 13. Power and efficiency as functions of the accelerating voltage for three values of body potential: (i) 33 kV, (ii) 33.8 kV, and (iii) 34.4 kV.

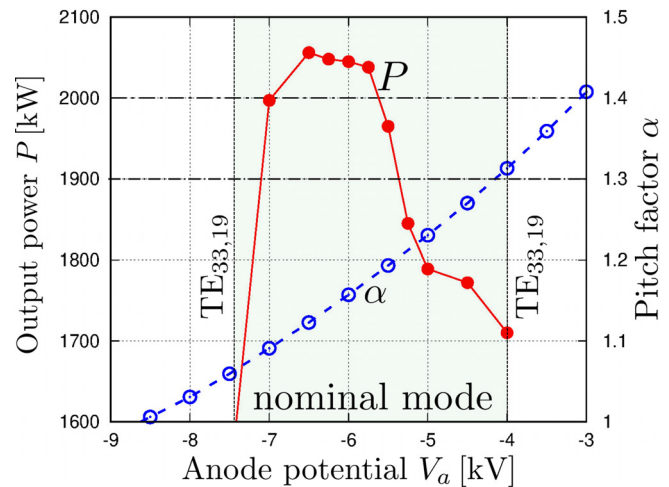


FIG. 14. Measured power and the theoretical value of the pitch factor as a function of the anode potential.

in the range of nominal value $I_b = 75$ A. Modifying the anode voltage independently, it was possible to optimize the pitch factor for a specific operating point. As shown in Fig. 14, a power higher than 2 MW was achieved when the theoretical value of the pitch factor α ranges between 1.1 and 1.2. For pitch factor values less than 1.1 and higher than 1.3, the competitor mode $TE_{33,19}$ is excited instead of the nominal one ($TE_{34,19}$).

These first experimental results are very promising since the gyrotron operation was not really optimized yet. In the near future, the gyrotron will be baked out and then, more systematic studies will be performed in short and longer pulses.

IV. CONCLUSION

Taking into account the recent understanding of the physics of the electron trapping mechanisms in the MIG region and the emitter ring manufacturing tolerances sensitivity on the electron beam quality, a new triode MIG for the 2 MW, 170 GHz modular coaxial cavity gyrotron has been designed at KIT and manufactured by TED. This MIG incorporates several novelties. An emitter ring with anti-emission coated ends was used for the suppression of the influence of the emitter ring radial deviation on the quality of the generated electron beam. It was theoretically shown that this sensitivity is more crucial in the triode configurations than the diode ones. In addition, the design criteria for the suppression of the electron trapping mechanisms were also taken into account, while the design of the new MIG ensures high beam quality in a large variety of magnetic field profiles.

Furthermore, a methodology was proposed in order to take the advantages of the operation with a triode MIG using only two power supplies without a significant limitation on the gyrotron performance and efficiency. The use of this method could be also extended to cases in which pitch factor adjustment is necessary for the gyrotron operation such as in multi-frequency and in step-tunable gyrotrons.

Finally, the first short-pulse experiments of the coaxial cavity gyrotron with the new MIG are also presented. A special procedure was introduced in order to operate the gyrotron with the unexpected

strong variation of the beam current during the first milliseconds of the pulse. A power higher than 2 MW was experimentally measured.

ACKNOWLEDGMENTS

This work has been carried out within the framework of the EUROfusion Consortium and has received funding from the Euratom research and training programme 2014–2018 and 2019–2020 under Grant Agreement No. 633053. The views and opinions expressed herein do not necessarily reflect those of the European Commission. The authors would like to warmly thank Professor I. Vomvoridis, Professor Q. M. Tran, Dr. J.-P. Hogge, and Dr. S. Alberti for fruitful discussions.

A part of the simulations was performed on the EUROfusion High Performance Computer (Marconi-Fusion).

REFERENCES

- ¹C. T. Iatrou, S. Kern, and A. B. Pavelyev, “Coaxial cavities with corrugated inner conductor for gyrotrons,” *IEEE Trans. Microwave Theory Tech.* **44**, 56 (1996).
- ²S. N. Vlasov, L. I. Zagryadskaya, and I. M. Orlova, “Open coaxial resonators for gyrotrons,” *Radio Eng. Electron. Phys.* **21**, 96–102 (1976).
- ³V. A. Flyagin, V. I. Khizhnyak, V. N. Manuilov, M. A. Moiseev, A. B. Pavelyev, V. E. Zapevalov, and N. A. Zavolsky, “Investigations of advanced coaxial gyrotrons at IAP RAS,” *Int. J. Infrared Millimeter Waves* **24**(1), 1–17 (2003).
- ⁴B. Piosczyk, G. Dammertz, O. Dumbrajs, O. Drumm, S. Illy, J. Jin, and M. Thumm, “A 2-MW, 170-GHz coaxial cavity gyrotron,” *IEEE Trans. Plasma Sci.* **32**, 413 (2004).
- ⁵T. Rzesnicki, G. Gantenbein, S. Illy, J. Jelonnek, J. Jin, I. Gr. Pagonakis, B. Piosczyk, A. Schlaich, and M. Thumm, “2 MW, 170 GHz coaxial-cavity short-pulse gyrotron—Investigations on electron beam instabilities and parasitic oscillations,” in 38th International Conference on Infrared, Millimeter, and Terahertz Waves (IRMMW-THz), Mainz, Germany, 14–19 September 2013.
- ⁶T. Rzesnicki, B. Piosczyk, S. Kern, S. Illy, J. Jin, A. Samartsev, A. Schlaich, and M. Thumm, “2.2-MW record power of the 170-GHz European preprototype coaxial-cavity gyrotron for ITER,” *IEEE Trans. Plasma Sci.* **38**, 1141–1149 (2010).
- ⁷T. Rzesnicki, G. Gantenbein, J. Jelonnek, J. Jin, I. Gr. Pagonakis, B. Piosczyk, A. Samartsev, A. Schlaich, and M. Thumm, “2 MW, 170 GHz coaxial-cavity short-pulse gyrotron—Single stage depressed collector operation,” in 2014 39th International Conference on Infrared, Millimeter, and Terahertz Waves (IRMMW-THz), Tucson, AZ, 14–19 September 2014.
- ⁸S. Ruess, K. A. Avramidis, M. Fuchs, G. Gantenbein, Z. Ioannidis, S. Illy, J. Jin, P. C. Kalaria, T. Kobarg, I. Gr. Pagonakis, T. Ruess, T. Rzesnicki, M. Schmid, M. Thumm, J. Weggen, A. Zein, and J. Jelonnek, “KIT coaxial gyrotron development: From ITER towards DEMO,” *Int. J. Microwave Wireless Technol.* **10**(Special Issue 5–6), 547–555 (2018).
- ⁹P. C. Kalaria, M. George, S. Illy, K. A. Avramidis, G. Gantenbein, S. Ruess, M. Thumm, and J. Jelonnek, “Multi-physics modelling of insert cooling system for an 170 GHz, 2 MW long-pulse coaxial-cavity gyrotron,” *IEEE Trans. Electron Devices* **66**, 4008–4015 (2018).
- ¹⁰J. Ph. Hogge, F. Albajar, S. Alberti, P. Benin, T. Bonicelli, S. Cirant, D. Fasel, T. Goodman, S. Illy, S. Jawla, C. Liévin, I. Gr. Pagonakis, A. Perez, B. Piosczyk, T. Rzesnicki, M. Thumm, and M. Q. Tran, “The European 2 MW, 170 GHz coaxial cavity gyrotron for ITER,” in 32th Joint International Conference on Infrared and Millimeter Waves and 15th International Conference on Terahertz Electronics, Conference Digest, Cardiff, UK, 2–7 September (2007), pp. 38–40.
- ¹¹J. Jelonnek, F. Albajar, S. Alberti, K. Avramidis, P. Benin, T. Bonicelli, F. Cismondi, V. Erckmann, G. Gantenbein, K. Hesch, J.-P. Hogge, S. Illy, Z. C. Ioannidis, J. Jin, H. Laqua, G. P. Latsas, F. Legrand, G. Michel, I. Gr. Pagonakis, B. Piosczyk, Y. Rozier, T. Rzesnicki, I. Tigelis, M. Thumm, M.-Q. Tran, and J. L. Vomvoridis, “From series production of gyrotrons for W7-X toward EU-1MW gyrotrons for ITER,” *IEEE Trans. Plasma Sci.* **42**, 1135 (2014).
- ¹²J. P. Hogge, T. P. Goodman, S. Alberti, F. Albajar, K. A. Avramidis, P. Benin, S. Bethuys, W. Bin, T. Bonicelli, A. Bruschi, S. Cirant, E. Droz, O. Dumbrajs, D. Fasel, F. Gandini, G. Gantenbein, S. Illy, S. Jawla, J. Jin, S. Kern, P. Lavanchy, C. Lievin, B. Marletaz, P. Marmillod, A. Perez, B. Piosczyk, I. Pagonakis, L. Porte, T. Rzesnicki, U. Siravo, M. Thumm, and M. Q. Tran, “First experimental results from the European Union 2-MW coaxial cavity ITER gyrotron prototype,” *Fusion Sci. Technol.* **55**, 204 (2009).
- ¹³I. Gr. Pagonakis, J.-P. Hogge, T. Goodman, S. Alberti, B. Piosczyk, S. Illy, T. Rzesnicki, S. Kern, and C. Lievin, “Gun design criteria for the refurbishment of the first prototype of the EU 170GHz/2MW/CW coaxial cavity gyrotron for ITER,” in 34th International Conference on Infrared, Millimeter and Terahertz Wave, Conference Proceedings, Busan, Korea, 21–25 September, 2009.
- ¹⁴Sh. E. Tsimring and V. E. Zapevalov, “Experimental study of intense helical electron beams with trapped electrons,” *Int. J. Electron.* **81**, 199 (1996).
- ¹⁵V. N. Manuilov and S. A. Polushkin, “Behavior of helical electron beams in gyrotrons with high pitch factors,” *Radiophys. Quantum Electron.* **52**, 714 (2009).
- ¹⁶I. Gr. Pagonakis, B. Piosczyk, J. Zhang, S. Illy, T. Rzesnicki, J.-P. Hogge, K. Avramidis, G. Gantenbein, M. Thumm, and J. Jelonnek, “Electron trapping mechanisms in magnetron injection guns,” *Phys. Plasmas* **23**, 023105 (2016).
- ¹⁷I. Gr. Pagonakis, S. Illy, and M. Thumm, “Influence of emitter ring manufacturing tolerances on electron beam quality of high power gyrotrons,” *Phys. Plasmas* **23**, 083103 (2016).
- ¹⁸I. Gr. Pagonakis, F. Albajar, S. Alberti, K. Avramidis, T. Bonicelli, F. Braummüller, A. Bruschi, I. Chelis, F. Cismondi, G. Gantenbein, V. Hermann, K. Hesch, J.-P. Hogge, J. Jelonnek, J. Jin, S. Illy, Z. Ioannidis, T. Kobarg, G. Latsas, F. Legrand, M. Lontano, B. Piosczyk, Y. Rozier, T. Rzesnicki, C. Schlatter, M. Thumm, I. Tigelis, M.-Q. Tran, T.-M. Tran, J. Weggen, and J. L. Vomvoridis, “Status of the development of the EU 170 GHz/1 MW/CW gyrotron,” *Fusion Eng. Des.* **96–97**, 149 (2015).
- ¹⁹T. Rzesnicki, I. Gr. Pagonakis, A. Samartsev, K. Avramidis, G. Gantenbein, S. Illy, J. Jelonnek, J. Jin, C. Lechte, M. Losert, B. Piosczyk, M. Thumm, and EGYC Team, “Recent experimental results of the European 1 MW, 170 GHz short-pulse gyrotron prototype for ITER,” in 40th International Conference on Infrared, Millimeter, and Terahertz Waves (IRMMW-THz 2015), Hong Kong, China, 23–28 August 2015.
- ²⁰Z. C. Ioannidis, T. Rzesnicki, F. Albajar, S. Alberti, K. A. Avramidis, W. Bin, T. Bonicelli, A. Bruschi, J. Chelis, P.-E. Frigot, G. Gantenbein, V. Hermann, J.-P. Hogge, S. Illy, J. Jin, J. Jelonnek, W. Kasperek, G. Latsas, C. Lechte, F. Legrand, T. Kobarg, I. Gr. Pagonakis, Y. Rozier, C. Schlatter, M. Schmid, I. G. Tigelis, M. Thumm, M. Q. Tran, A. Zein, and A. Zisis, “CW experiments with the EU 1 MW, 170 GHz industrial prototype gyrotron for ITER at KIT,” *IEEE Trans. Electron Devices* **64**, 3885–3892 (2017).
- ²¹B. Piosczyk, “A novel 4.5-MW electron gun for a coaxial cavity gyrotron,” *IEEE Trans. Electron Devices* **48**, 2938 (2001).
- ²²I. Gr. Pagonakis, K. A. Avramidis, G. Gantenbein, S. Illy, Z. Ioannidis, F. Legrand, S. Ruess, T. Ruess, T. Rzesnicki, M. Thumm, and J. Jelonnek, “Magnetron injection gun for the 2 MW 170 GHz modular coaxial cavity gyrotron,” in 43rd International Conference on Infrared, Millimeter, and Terahertz Waves, Nagoya, Japan, 9–14 September, 2018.
- ²³V. K. Lygin, V. N. Manuilov, A. N. Kuftin, A. B. Pavelyev, and B. Piosczyk, “Inverse magnetron injection gun for a coaxial 1.5 MW, 140GHz, gyrotron,” *Int. J. Electron.* **79**, 227 (1995).
- ²⁴S. Ruess, I. Gr. Pagonakis, G. Gantenbein, S. Illy, T. Kobarg, T. Rzesnicki, M. Thumm, J. Weggen, and J. Jelonnek, “An inverse magnetron injection gun for the KIT 2-MW coaxial-cavity gyrotron,” *IEEE Trans. Electron Devices* **63**(5), 2104–2109 (2016).
- ²⁵I. Gr. Pagonakis, K. A. Avramidis, G. Gantenbein, T. Rzesnicki, A. Samartsev, and J. Jelonnek, “Magnetic field profile analysis for experimental gyrotron investigation,” *Phys. Plasmas* **24**, 033102 (2017).
- ²⁶Y. Yamaguchi, Y. Tatsumatsu, and T. Saito, “Influence of thermal-insulation structure of thermionic cathode on oscillation efficiency of a sub-THz gyrotron,” in 41st International Conference on Infrared, Millimeter, and Terahertz Waves, Conference Proceedings, Copenhagen, Denmark, 25–30 September, 2016.
- ²⁷I. Gr. Pagonakis, S. Illy, T. Rzesnicki, Z. Ioannidis, K. A. Avramidis, G. Gantenbein, T. Kobarg, B. Piosczyk, M. Thumm, and J. Jelonnek, “Numerical investigation on spent beam deceleration schemes for depressed collector of a high power gyrotron,” *IEEE Trans. Electron Devices* **65**(6), 2321–2326 (2018).